R. & M. No. 2766
(12,605)
A.R.C. Technical Report

MINISTRY OF SUPPLY

AERONAUTICAL RESEARCH COUNCIL
REPORTS AND MEMORANDA

The Initial Buckling of a Long and Slightly bowed Panel under Combined Shear and Normal Pressure

By

E. H. BROWN, B.Sc.(Eng.)
and
H. G. HOPKINS, M.Sc., A.F.R.Ae.S.

LONDON: HER MAJESTY'S STATIONERY OFFICE
1953
SIX SHILLINGS NET

The Initial Buckling of a Long and Slightly bowed Panel under Combined Shear and Normal Pressure

By

E. H. Brown, B.Sc.(Eng.) and H. G. Hopkins, M.Sc., A.F.R.Ae.S.

Communicated by the Principal Director of Scientific Research (Air), Ministry of Supply

Reports and Memoranda No. 2766*
June, 1949

Summary.—Recent American experimental work has suggested that the resistance to buckling of wing skin panels under compression or shear loads is improved by aerodynamic suction. A complete theoretical analysis of this problem is very difficult, because compression load necessarily involves the consideration of post-buckling behaviour. An approach is made in this report by considering the restricted problem of the initial buckling of a long, thin and slightly bowed panel under combined shear and normal pressure.

The theoretical values of the initial shear buckling stress, which agree well with American experimental values increase with both pressure and curvature; the wavelength of the buckles also increases with pressure, but decreases with curvature. The difference between the buckling stresses for simply supported and clamped edges is considerable for a flat panel under shear alone but decreases rapidly with curvature and pressure, thus making the indeterminacy of practical edge conditions of less importance.

---

1. *Introduction.*—Recent American work[1 to 4] has shown that aerodynamic suction may be expected to improve the resistance of wing skin panels to buckling under compression or shear loads. A complete theoretical analysis of the general combined loading problem is very difficult, because compression buckling is only satisfactorily discussed in terms of the post-buckling behaviour of the skin. Moreover the pre-buckling stress distribution in the practical case is complicated by ballooning between the wing ribs, giving a surface with variable double curvature.

As an approach to the general problem, the present report gives an analytical account of the stability under combined normal pressure and shear of a long and slightly bowed panel. This could be considered as part of a circular cylinder of great radius, so that the present problem would appear to be covered by R. & M. 2423[5], but unfortunately Donnell's analysis[6], upon which R. & M. 2423[5] is based, is not easily extended to take account of normal pressure for low degrees of curvature, and only the extension for fuselage or engine nacelle curvatures was attempted. On the other hand the present analysis is not readily applicable to high degrees of curvature, for the computation involved becomes excessive. R. & M. 2423[5] and this report together cover the complete range.

2. *Statement of Problem and Method of Solution.*—The panel is assumed to be sufficiently long for the conditions over the short edges to be neglected as far as buckling is concerned, so that the wavelength may be considered a continuous variable; *i.e.*, the length of the panel is not less than three times the wavelength.† The long edges have a constant curvature, of the same order as that of an inter-spar wing panel; the short edges are straight.

The shear stress is uniformly applied along the edges and the normal pressure is uniformly distributed over one face. It is assumed that the stresses do not exceed the limit of proportionality of the material.

---

* R.A.E. Report Structures 42, received 3rd October, 1949.

† Note that the wave length increases with the pressure (*see* section 5.3).

Until the incidence of buckling, normal displacements of the curved edges as well as relative axial and circumferential movements are permitted, so that the pressure is resisted by a uniform hoop stress with reactions at the short edges. During buckling all translational displacements of the curved edges are prevented and they are taken to be either simply-supported or clamped. This is not strictly the case of an aircraft wing panel, where before buckling normal displacements of the curved edges are resisted by ribs, giving inter-rib ballooning, and relative axial movements are resisted by the wing spars. To ignore these restrictions on the displacements is equivalent to freeing the panel from certain constraints, so that the resulting critical stress will be an under-estimate of the practical case. To take the restrictions into account is to complicate the problem with a variable double curvature due to the ballooning and a non-uniform pre-buckling stress distribution, and the consequent non-linear equations present formidable analytical difficulties. The seriousness of this under-estimate of the practical buckling stress can only be gauged, in the absence of a completely rigorous solution, by comparison with experiments; a comparison with such experimental results as exist is given in section 6.

The theoretical analysis (which is given in full in the Appendix) is an extension of the work of Leggett (R. & M. 1972[7]) on the initial buckling of a slightly bowed panel under shear alone, and it consists of an exact solution of the basic stability equations.

3. *Notation.*—

a	Width of panel, measured along the short straight edges (in.)	
b	Length of panel, measured along the long curved edges (in.)	
$2h$	Thickness of panel (in.)	
r	Radius of curvature of panel, assumed uniform (in.)	
E	Young's modulus (lb/in.^{2}),	
ν	Poisson's ratio, assumed to be $0 \cdot 3$,	
q	Normal pressure (or aerodynamic suction) (lb/in.^{2})	
q_0	Critical normal pressure when there is no shear stress (negative because the normal pressure is assumed to be positive when it acts outwards) (lb/in.^{2})	
τ	Critical shear stress (lb/in.^{2})	
τ_0	Critical shear stress when there is no normal pressure (lb/in.^{2})	
λ	Wavelength (in.)	
θ	Angle between the curved edges of the panel and the direction of a wave-crest (or -trough), measured at a point midway between the curved edges of the panel and remote from the straight edges,	
θ_0	Value of θ when $\underline{q} = 0$	
α	Angle between the curved edges of the panel and the direction of the principal tensile stress at a point remote from the straight edges,	
α_0	Value of α when $\underline{q} = 0$	
$k =$	$\{3(1 - \nu^2)/\pi^4\}^{1/2}(a^2/rh)$	curvature parameter,
$\underline{q} =$	$\{3(1 - \nu^2)/2\pi^2\}(a^2r/h^3)(q/E)$	pressure parameter,
$\bar{\tau} =$	$\{6(1 - \nu^2)/\pi^2\}(a^2/h^2)(\tau/E)$	shear stress parameter,
$\bar{\lambda} =$	λ/a	wavelength parameter.

4. *Summary of Previous Experimental and Theoretical Work.*—The effect of normal pressure on the stability of thin-walled circular cylinders under torsion has been investigated experimentally and theoretically by Crate, Batdorf and Baab[1] who found that the critical shear stress was appreciably raised by the pressure. These authors, who appear to be the first to consider the problem theoretically, derive the following interaction formula,

$$(\tau/\tau_0)^2 + q/q_0 = 1,$$

and this agrees well with their experimental results. Their analysis is somewhat empirical and provides no information on the length or angle of waves. For this reason the present writers investigated the problem in a more fundamental way (R. & M. 2423[5]) which is based on the work of Donnell[6] on the stability of thin-walled circular tubes under torsion. The values of the critical stress so obtained are in good agreement with the experimental and theoretical results of Ref. 1. In addition the analysis provides information on the variation of the length and angle of waves with normal pressure.

The effect of normal pressure on the buckling of thin and slightly curved sheet under shear has been investigated experimentally by Rafel and Sandlin[3, 4] who also found that normal pressure markedly improves the resistance to buckling. Their experiments were made on specimens which were clearly designed to simulate a section of the inter-spar region of a stressed-skin wing and were essentially torsion-box structures of 24 S-T aluminium alloy. The skin was stabilised only by chordwise ribs, there being no spanwise stringers. A diagrammatic sketch, adapted from Fig. 3 of Ref. 4, of a typical test specimen and the method of applying end load is shown in Fig. 6. Some, but not all, of the specimens had a degree of curvature within the range considered here, and in addition had a large enough length to width ratio. Where this is the case it is possible to make a comparison between experimental values of critical stresses and those predicted by the present theory. The experimental shear buckling loads correspond to the first signs of buckling and were determined by instrumental means; the post-buckling behaviour of the sheet was not considered. Unfortunately, Refs. 3 and 4 give no data on the variation of length or angle of waves with normal pressure, nor on the increased distortion due to increased shear and pressure beyond the critical values.

Future experimental work should consider the influence of normal pressure on the post-buckling behaviour of thin curved sheet under combined compression and shear loads. This would be of great assistance in theoretical work on the combined loading case, which has most application in practice.

5. *Discussion of Results.*—5.1. *Presentation.*—The results are expressed in terms of certain non-dimensional parameters, k, $\bar{q}$, $\bar{\tau}$, and $\bar{\lambda}$, referred to as the curvature, pressure, critical shear stress and wavelength parameters respectively. The critical shear stress and wavelength parameters are functions of the curvature and pressure parameters and the type of edge support. The range of parameters considered adequately covers application to wing design, and is

$$0 \leqslant k \leqslant 5, \quad 0 \leqslant \bar{q} \leqslant 50.$$

5.2. *Critical Shear Stress.*—The variation of the critical shear stress parameter with the curvature and pressure parameters is given in Tables 1 and 2 for simply supported and clamped edges respectively.

The results show clearly that the critical shear stress is greatly increased by normal pressure, and the curves in Figs. 2 and 3 also show that there is an approximately linear variation of $\bar{\tau}$ with k for a given value of $\bar{q}$, this being more marked for simply supported than for clamped edges. Further, the difference between the critical shear stresses for the two types of edge support, considerable when the panel is flat and there is no normal pressure, diminishes rapidly with increasing curvature and normal pressure. This observation is of considerable importance, because although the practical edge conditions usually approximate to simple support their indeterminacy is not now of great account. In any event the assumption of simple support will lead to an underestimate of the critical stress. As an illustration it is found that for a long flat panel under shear alone ($k = \bar{q} = 0$) the critical shear stress for clamped edges is 70 per cent in excess of that for simply supported edges, but that when $k = 5$ and $\bar{q} = 50$ the excess is only 12 per cent.

5.3. *Wavelength.*—The variation of the wavelength parameter with the curvature and pressure parameters is shown in Figs. 4 and 5, and numerical values are given in Table 3.

For a given pressure and curvature the wavelength for simply supported edges always exceeds that for clamped edges, and, for both types of edge support, the wavelength increases with pressure and decreases with curvature. In the case of a flat panel under shear alone, the wavelength for clamped edges is 67 per cent of that for simply supported edges, but when $k = 5$, $\bar{q} = 0$ and $k = 5$, $\bar{q} = 50$ the corresponding figures are 92 per cent and 91 per cent respectively; hence the difference in the wavelengths for the types of edge support falls considerably with increased curvature but is little affected by pressure.

These results differ from those of R. & M. 2423[5]. The wavelength then was found to increase with the pressure, while the difference between the wavelengths for the two types of edge support decreased.

5.4. *Angle of Waves.*—The angle of waves is defined as the angle between the curved edges and the direction of a wave-crest (or -trough) measured at a point midway between the curved edges and remote from the straight edges. The method of analysis does not readily give the angle of waves, but it is possible to get an approximate prediction from simple physical considerations.

The direction of waves is approximately parallel to the direction of the principal tensile stress which makes an angle α with the curved edges. It is known that for the special case of a long flat panel under shear alone the angle of waves, θ_0, is 43 deg and 39 deg for simply supported and clamped edges respectively[8], while $\alpha_0 = 45$ deg. An approximate expression for the angle of waves is therefore

$$\theta = \frac{4\alpha}{\pi}\,\theta_0 .$$

The normal pressure induces a tensile stress of $qr/2h$ lb/in.^{2} in the panel parallel to the curved edges and consequently

$$\tan 2\alpha = 4\tau h/qr ,$$

which gives

$$\theta = (2\theta_0/\pi)\,\tan^{-1}\,(4\tau h/qr) .$$

The results in Ref. 6 suggest that θ_0 falls approximately linearly with an increase in curvature, giving a reduction of 40 per cent and 25 per cent for simply supported and clamped edges respectively when $k = 5$.

5.5. *Accuracy.*—The analysis given in the Appendix is an exact solution of the basic stability equations, which are valid provided that the ratios h^2/a^2 and a^2/r^2 are small in comparison with unity. Both of these conditions are satisfied for a wing surface panel.

It is emphasised that no account has been taken of the post-buckling behaviour of the panel. Leggett and Jones (R. & M. 2190[9]) who have investigated the post-buckling behaviour of a thin circular cylinder under axial compression, show that the cylinder can be maintained in a well-buckled form by a compressive end-load of approximately one third of the classical initial buckling load. They conclude that, due to the inevitable initial imperfections in specimens, the buckling load achieved under test conditions will lie between the classical initial buckling load and the least load that can maintain the structure in a buckled form. Their theoretical results are in very fair agreement with experiment. This difference which so often exists between the classical buckling load and that achieved in test is much smaller for the case of torsion loading than for compression. It is therefore probable that a theoretical treatment analogous to that of Leggett and Jones would indicate a similar (though much smaller) effect of inital imperfections upon the critical shear stress.

In general, practical edge conditions will be intermediate to the two cases considered, approximating to simple support. As the difference between the theoretical critical stresses for the two types of support diminishes with increasing curvature and pressure (*see* section 5.2) it follows that the assumption of simply supported edges, leading to a slight underestimate of the stress, will be quite satisfactory in practical applications. The panel is assumed to be long, so that the support along the short edges may be neglected and the wavelength be considered a continuous variable. This assumption is generally valid when the length of the panel exceeds three times the wavelength. Once again deviation from the ideal condition leads to an underestimate of the critical stress.

It finally remains to consider the accuracy of the computation. The critical shear stress is given in terms of the roots of an infinite determinantal equation which is intractable as it stands. Attention is therefore confined to a finite determinantal equation corresponding to the most important part of the distortion that takes place during buckling, and the least critical stress and the associated wavelength can be found to any degree of accuracy by consideration of a determinant of a sufficiently high order. The computation, however, increases rapidly with the determinant order and it is not practicable, or indeed necessary, to deal with determinants above the fourth order. For the most part third-order determinants have been considered, but in certain selected cases the computation is carried to the fourth order, although the work involved makes even this generally impracticable. The accuracy of the results must be gauged from the rapidity of convergence with increase in the order of the determinantal equation. It is estimated that, for the range considered, the error in the critical stress obtained from the third-order determinantal equation never exceeds 4 per cent for simply supported edges or 7 per cent for clamped edges.

6. *Comparison between Theoretical and American Experimental Values of the Critical Shear Stress.*—Details of the construction of the test specimens used by Rafel and Sandlin[3,4] are given in Ref. 4, but it is important to notice here that the skin was stabilised by ribs alone and was attached to the spar and rib flanges by single rows of rivets. Ref. 3 only describes work on two specimens, the major difference between these being in the rib pitch which was 10 in. for one and 30 in. for the other; Ref. 4 covers a much more extensive field and in all twenty specimens were tested under combined shear and normal pressure. The rib pitches and skin radii of curvature were various, giving b/a ratios from 3 to $0 \cdot 75$ and $r/2h$ ratios from ∞ to 400. In all cases the maximum normal pressure was 6 lb/in.^{2}. Of the twenty-two specimens altogether tested under combined shear and normal pressure only three have dimensions such that an immediate comparison may be made with the present report, and in order to obtain a wider comparison special computations have been made for a further three specimens for which $k > 5$. The skin panels of five of these six specimens have a b/a ratio of 3, and the remaining one a ratio of $1 \cdot 5$. The relevant dimensions and particulars of the six specimens are given in Table 4.

The detailed comparison between experiment and theory is shown in Fig. 7. The agreement is good for panels Nos. 2, 3 and 4; the agreement for panels Nos. 1 and 5 is good for pressures up to 2 lb/in.^{2}, but above this pressure the experimental value remains sensibly constant and eventually falls below that predicted theoretically. The probable explanation of this discrepancy is that any small initial irregularities become increasingly pronounced with the repeated application of load, and accordingly the resistance of the panel to buckling progressively deteriorates. The comparison for panel No. 6 is interesting; here the b/a ratio of the panel is $1 \cdot 5$ as against 3 for the other panels. It is therefore to be expected that the theoretical value of the critical stress will underestimate the experimental value. This is precisely what the comparison shows, but the underestimate is small at low pressures and appears to increase slightly with the pressure. The two theoretical curves for this specimen lie close together because of the relatively high value of the curvature parameter.

The agreement between these experiments and the theory is therefore quite satisfactory, and it is seen that the theoretical value of the critical shear stress for simply supported edges is a slight underestimate of the experimental value.

Refs. 3 and 4 give no details of the length or angle of waves and it is not therefore possible to make any comparison with theory.

7. *Conclusions.*—The theoretical values of the initial shear buckling stress agree well with American experimental values, despite the theory's neglect of the considerable inter-rib ballooning which must have occurred in the experiments. The critical shear stress increases slowly with curvature and sharply with normal pressure over the range considered. The wave-length of the buckles decreases with curvature but increases with pressure; no experimental results are yet available for this. The difference between the buckling stresses for simply supported and clamped edges is considerable for a flat panel under shear alone but decreases rapidly with curvature and pressure, thus making the indeterminacy of practical edge conditions of less importance.

Future experimental work should consider the influence of normal pressure on the post-buckling behaviour of thin curved sheet under combined compression and shear loads. This would be of great assistance in theoretical work on the combined loading case.

Acknowledgement.—The authors are indebted to Miss G. M. Chitty for undertaking the major part of the computation.

REFERENCES

No.	*Author.*	*Title, etc.*
1	H. Crate, S. B. Batdorf, and G. W. Baab	The Effect of Internal Pressure on the Buckling Stress of Thin-Walled Circular Cylinders under Torsion. N.A.C.A. Report No. L4E27. May, 1944.
2	N. Rafel	Effect of Normal Pressure on the Critical Compression Stress of Curved Sheet. N.A.C.A. Bulletin. November, 1942.
3	N. Rafel	Effect of Normal Pressure on the Critical Shear Stress of Curved Sheet. N.A.C.A. Bulletin. January, 1943.
4	N. Rafel and C. W. Sandlin ..	Effect of Normal Pressure on the Critical Compressive and Shear Stress of Curved Sheet. N.A.C.A. Report No. L5B10. March, 1945.
5	H. G. Hopkins and E. H. Brown ..	The Effect of Internal Pressure on the Initial Buckling of Thin-Walled Circular Cylinders under Torsion. R. & M. 2423. January, 1946.
6	L. H. Donnell	Stability of Thin-Walled Tubes under Torsion. N.A.C.A. Report No. 479. 1933.
7	D. M. A. Leggett	The Initial Buckling of Slightly Curved Panels under Combined Shear and Compression. R. & M. 1972. December, 1943.
8	R. V. Southwell and S. W. Skan ..	On the Stability under Shearing Forces of a Flat Elastic Strip. *Proc. Roy. Soc.*, Series A, Vol. 105, pp. 582-607. 1924.
9	D. M. A. Leggett and R. P. N. Jones	The Behaviour of a Cylindrical Shell under Axial Compression when the Buckling Load has been Exceeded. R. & M. 2190. August, 1942.
10	Dean, W. R.	On the Theory of Elastic Stability. *Proc. Roy. Soc.*, Series A, Vol. 107, pp. 734-760. 1925.

APPENDIX I

Theoretical Analysis

1. *Introduction.*—The analysis is a development of that given by Leggett (R. & M. 1972[7]) for the associated problem with shear loading alone. Inevitably parts of the present analysis duplicate parts of Leggett's paper, but various changes in the notation have been made both for convenience and in order to present the analysis as concisely as possible.

2. *Notation.*—Notation, in addition to that already given, is:—

x, y, z	Axial, circumferential and radial orthogonal curvilinear co-ordinates
$\xi = \pi x/a$	Non-dimensional axial co-ordinate
$\eta = \pi y/a$	Non-dimensional circumferential co-ordinate
u_0, v_0, w_0	Axial, circumferential and radial displacements of points in the middle surface immediately before buckling,
u', v', w'	Axial, circumferential and radial displacements of points in the middle surface during buckling,
$\sigma_x, \sigma_y, \tau_{xy}$	Stresses in the middle surface
ϕ	Stress function

3. *Co-ordinate System and Displacements.*—The system of orthogonal curvilinear co-ordinates and the corresponding displacements are shown in Fig. 1. Attention is confined throughout to the middle surface. One of the curved edges and the generator through its mid-point are taken as y- and x-axes respectively, so that the edges are given by

$$x = 0, a \text{ and } y = \pm b/2$$

or

$$\xi = 0, \pi \text{ and } \eta = \pm \pi b/2a.$$

The third co-ordinate axis z, which is directed along the inward-drawn normal at any point, is chosen so that x, y, z form a right-handed system. The faces of the panel are then given by

$$z = \pm h.$$

The displacements corresponding to the co-ordinates x, y, z are u, v, w respectively.

4. *Derivation of Basic Stability Equations.*—Under the conditions set out in section 2 of the main report, the state of stress immediately before buckling is given by

$$\sigma_x = 0, \quad \sigma_y = qr/2h, \quad \tau_{xy} = \tau, \qquad (1)$$

and the corresponding displacements are

$$u_0 = -\nu qrx/2Eh, \quad v_0 = 2(1 + \nu)\tau x/E, \quad w_0 = -qr^2/2Eh \qquad (2)$$

which may be shown to satisfy Dean's shell equations of equilibrium[10].

If the panel is about to buckle the shell equations are also satisfied by the displacements

$$u_0 + u', \quad v_0 + v', \quad w_0 + w' \qquad (3)$$

where u', v', w' are arbitrarily small but not all zero.

The basic stability equations are obtained by the subtraction of the two sets of shell equations which correspond to the displacements u_0, v_0, w_0 and $u_0 + u'$, $v_0 + v'$, $w_0 + w'$, all product terms of the displacements u', v', w' being omitted so that the final equations are linear in these displacements. The equations are not set down here because in their present form they are unnecessarily complicated and may legitimately be simplified on the basis of certain assumptions. First, it is assumed that the middle-surface strains due to the displacements u', v', w' are of the same order of magnitude, and this implies that

$$O(u') = O(v') = (a/r)O(w').$$

Second, it is assumed that the ratios h^2/a^2, a^2/r^2 may be neglected in comparison with unity. The first assumption is correct from a physical standpoint and is clearly valid for the special case of a flat panel, for then u', v' are zero to the first order of small quantities. The second assumption is correct for a thin and slightly bowed panel. The basic stability equations are now

$$\frac{\partial}{\partial x}\left\{\frac{\partial u'}{\partial x} + \nu\left(\frac{\partial v'}{\partial y} - \frac{w'}{r}\right)\right\} + \frac{1-\nu}{2}\,\frac{\partial}{\partial y}\left\{\frac{\partial v'}{\partial x} + \frac{\partial u'}{\partial y}\right\} = 0, \quad \ldots \quad (4)$$

$$\frac{1-\nu}{2}\,\frac{\partial}{\partial x}\left\{\frac{\partial v'}{\partial x} + \frac{\partial u'}{\partial y}\right\} + \frac{\partial}{\partial y}\left\{\left(\frac{\partial v'}{\partial y} - \frac{w'}{r}\right) + \nu\,\frac{\partial u'}{\partial x}\right\} = 0, \quad \ldots \quad (5)$$

$$\frac{h^2}{3}\,\nabla_1^4 w' - 2(1-\nu^2)\,\frac{\tau}{E}\,\frac{\partial^2 w'}{\partial x\,\partial y} - \frac{1-\nu^2}{2}\,\frac{qr}{Eh}\,\frac{\partial^2 w'}{\partial y^2} - \frac{1}{r}\left\{\left(\frac{\partial v'}{\partial y} - \frac{w'}{r}\right) + \nu\,\frac{\partial u'}{\partial x}\right\} = 0, \quad (6)$$

where

$$\nabla_1^2 \equiv \partial^2/\partial x^2 + \partial^2/\partial y^2;$$

and these equations may be re-written in the form

$$\frac{\partial}{\partial \xi}\left\{\frac{\partial u'}{\partial \xi} + \nu\left(\frac{\partial v'}{\partial \eta} - \frac{aw'}{\pi r}\right)\right\} + \frac{1-\nu}{2}\,\frac{\partial}{\partial \eta}\left\{\frac{\partial v'}{\partial \xi} + \frac{\partial u'}{\partial \eta}\right\} = 0, \quad \ldots \quad (7)$$

$$\frac{1-\nu}{2}\,\frac{\partial}{\partial \xi}\left\{\frac{\partial v'}{\partial \xi} + \frac{\partial u'}{\partial \eta}\right\} + \frac{\partial}{\partial \eta}\left\{\left(\frac{\partial v'}{\partial \eta} - \frac{aw'}{\pi r}\right) + \nu\,\frac{\partial u'}{\partial \xi}\right\} = 0, \quad \ldots \quad (8)$$

$$\frac{h^2}{3}\,\nabla_1^4 w' - \frac{2(1-\nu^2)}{\pi^2}\,\frac{\tau a^2}{E}\,\frac{\partial^2 w'}{\partial \xi\,\partial \eta} - \frac{(1-\nu^2)}{2\pi^2}\,\frac{qa^2 r}{Eh}\,\frac{\partial^2 w'}{\partial y^2} - \frac{a^3}{\pi^3 r}\left\{\left(\frac{\partial v'}{\partial \eta} - \frac{aw'}{\pi r}\right) + \nu\,\frac{\partial u'}{\partial \xi}\right\} = 0, \quad (9)$$

where now

$$\nabla_1^2 \equiv \partial^2/\partial \xi^2 + \partial^2/\partial \eta^2.$$

Only one term in the above equations involves the normal pressure, and it constitutes the sole difference between the basic stability equations for the present problem and those of R. & M. 1972[7].

5. *Solution of the Basic Stability Equations.*—The problem is to determine the solution of equations (7) to (9) for which the displacements u', v', w' are not all zero, are compatible, are periodic in the co-ordinate η and satisfy stipulated boundary conditions.

Equations (7) and (8) are satisfied identically by the introduction of a stress function ϕ such that

$$\frac{\partial u'}{\partial \xi} + \nu\left(\frac{\partial v'}{\partial \eta} - \frac{aw'}{\pi r}\right) = \pi\,\frac{\partial^2 \phi}{\partial \eta^2}, \quad \ldots \quad (10)$$

$$\frac{1-\nu}{2}\left(\frac{\partial v'}{\partial \xi} + \frac{\partial u'}{\partial \eta}\right) = -\pi\frac{\partial^2 \phi}{\partial \xi\,\partial \eta}, \qquad (11)$$

$$\left(\frac{\partial v'}{\partial \eta} - \frac{a w'}{\pi r}\right) + \nu\frac{\partial u'}{\partial \xi} = \pi\frac{\partial^2 \phi}{\partial \xi^2}. \qquad (12)$$

The displacements u', v' are next eliminated between equations (10) to (12) and between equations (9) and (12), to give the compatibility equation

$$\nabla_1^4\phi + S\frac{\partial^2 w'}{\partial \xi^2} = 0, \qquad (13)$$

and

$$\nabla_1^4 w' - T\frac{\partial^2 \phi}{\partial \xi^2} - \bar{\tau}\frac{\partial^2 w'}{\partial \xi\,\partial \eta} - \bar{q}\frac{\partial^2 w'}{\partial \eta^2} = 0, \qquad (14)$$

respectively, where

$$\left.\begin{aligned} S &= \frac{(1-\nu^2)}{\pi^2}\frac{a}{r} \\ T &= \frac{3a^3}{\pi^2 r h^2} \end{aligned}\right\} \qquad (15)$$

Both w' and ϕ must be periodic in η, and without restriction it is therefore legitimate to assume that

$$\left.\begin{aligned} w' &= w_1\cos m\eta + w_2\sin m\eta = (\mathrm{R})^*\{(w_1 + iw_2)\exp(-im\eta)\} \\ &= (\mathrm{R})\{W\exp(-im\eta)\}, \\ \phi &= \phi_1\cos m\eta + \phi_2\sin m\eta = (\mathrm{R})\{(\phi_1 + i\phi_2)\exp(-im\eta)\} \\ &= (\mathrm{R})\{\Phi\exp(-im\eta)\}, \end{aligned}\right\} \qquad (16)$$

where w_1, w_2, ϕ_1, ϕ_2 are real functions of ξ only and $2a/m$ is the wavelength. Related analytical expressions for W and Φ must now be found which are perfectly general, satisfy appropriate boundary conditions and may be differentiated term by term when their substitution into differential equations is necessary. From physical considerations it may be asserted that any differential coefficient of the radial displacement is a continuous function of ξ $(0 \leqslant \xi \leqslant \pi)$ and η $(-\infty < \eta < \infty)$. $d^4W/d\xi^4$ may therefore be expanded as a half-range Fourier sine series which will be valid in the range $0 < \xi < \pi$, that is

$$\frac{d^4W}{d\xi^4} = \sum_{t=1}^{\infty} A_t t^4 \sin t\xi, \quad (0 < \xi < \pi), \qquad (17)$$

where A_t is complex. The coefficient t^4 is introduced merely for convenience, and then from the convergence of Fourier series it is known that

$$|A_t| < M/t^5 \ (t = 1, 2, \ldots), \qquad (18)$$

where M is some constant independent of t. A Fourier series may legitimately be integrated term by term any finite number of times, and equation (17) may therefore be integrated to give the following expression for W,

$$W = \sum_{t=1}^{\infty} A_t \sin t\xi + E + F\xi + G\xi^2 + H\xi^3, \quad (0 \leqslant \xi \leqslant \pi), \qquad (19)$$

where E, F, G, H are arbitrary complex constants of integration.

---

* (R) = ‘ real part of ’

The radial displacement is accordingly

$$w' = (\mathrm{R}) \left[\left\{\sum_{t=1}^{\infty} A_t \sin t\xi + E + F\xi + G\xi^2 + H\xi^3\right\} \exp(-im\eta)\right], \quad (0 \leqslant \xi \leqslant \pi, \quad -\infty < \eta < \infty), \qquad (20)$$

this expression being perfectly general and legitimately differentiable term by term up to four times with respect to ξ. Substitution for ϕ and w' from equations (16) and (20) in equation (13) yields

$$\left(\frac{d^4}{d\xi^4} - 2m^2 \frac{d^2}{d\xi^2} + m^4\right)\Phi = S\left(\sum_{t=1}^{\infty} t^2 A_t \sin t\xi - 2G - 6H\xi\right), \qquad (21)$$

which on integration gives,

$$\Phi = S\left\{\sum_{t=1}^{\infty} t^2 A_t \sin t\xi/(t^2 + m^2)^2 - (2G + 6H\xi)/m^4\right\} + (A \cosh m\xi + B \sinh m\xi) + \xi(C \cosh m\xi + D \sinh m\xi), \qquad (22)$$

where A, B, C, D are arbitrary complex constants. Hence

$$\phi = (\mathrm{R}) \left\{\left[S\left\{\sum_{t=1}^{\infty} t^2 A_t \sin t\xi/(t^2 + m^2)^2 - (2G + 6H\xi)/m^4\right\} + (A \cosh m\xi + B \sinh m\xi) + \xi(C \cosh m\xi + D \sinh m\xi) \right] \exp(-im\eta)\right\}. \qquad (23)$$

Along each curved edge there are four boundary conditions to be satisfied, one for each of the axial and circumferential displacements and two for the radial displacement. Altogether there are therefore eight boundary conditions, and the eight arbitrary constants A, B, C, D, E, F, G, H are in general just sufficient to satisfy them.

5.1. *Simply Supported Edge Conditions.*—The boundary conditions here are

$$u' = v' = w' = \partial^2 w'/\partial\xi^2 = 0 \quad \text{for } \xi = 0, \pi \ (-\infty < \eta < \infty). \qquad (24)$$

The conditions for the radial displacement are satisfied if

$$E = F = G = H = 0. \qquad (25)$$

It is necessary next to express the remaining boundary conditions in terms of Φ and W. This is achieved by using equations (10) to (12) and (16), and the conditions are now

$$\left.\begin{aligned} \frac{d^2\Phi}{d\xi^2} + \nu m^2 \Phi &= 0 \qquad (26)\\ \frac{d^3\Phi}{d\xi^3} - (2 + \nu) m^2 \frac{d\Phi}{d\xi} + \frac{(1 - \nu^2)}{\pi^2} \frac{a}{\nu} \frac{dW}{d\xi} &= 0 \qquad (27) \end{aligned}\right\} \text{for } \xi = 0, \pi \ (-\infty < \eta < \infty),$$

These, together with equations (19) and (22), determine the arbitrary constants, A, B, C, D as follows:—

$$\left.\begin{aligned} AQ &= 2X\{(3 - \nu) \sinh m\pi \cosh m\pi + (1 + \nu)m\pi\} - 2Y\{(3 - \nu) \sinh m\pi + (1 + \nu)m\pi \cosh m\pi\},\\ BQ &= X\{(1 + \nu)^2 m^2\pi^2 - 2(3 - \nu) \sinh^2 m\pi\} - Y(1 - \nu^2)m\pi \sinh m\pi,\\ CQ &= X(1 + \nu)(3 - \nu)m \sinh^2 m\pi - Y(1 + \nu)^2 m^2\pi \sinh m\pi,\\ DQ &= -X(1 + \nu)m\{(3 - \nu) \sinh m\pi \cosh m\pi + (1 + \nu)m\pi\} + Y(1 + \nu)m\{(3 - \nu) \sinh m\pi + (1 + \nu)m\pi \cosh m\pi\}, \end{aligned}\right\} \qquad (28)$$

where

$$\left.\begin{aligned}
Q &= \frac{(1+\nu)m}{S}\{(3-\nu)^2 \sinh^2 m\pi - (1+\nu)^2 m^2\pi^2\}, \\
X &= \sum_{t=1}^{\infty} a_t A_t, \\
Y &= \sum_{t=1}^{\infty} (-)^t a_t A_t, \\
a_t &= t(\nu t^2 - m^2)/(t^2 + m^2)^2
\end{aligned}\right\} \quad \begin{matrix}(28)\\ \textit{continued}\end{matrix}$$

The expressions for w' and ϕ given by equations (20), (23), (25) and (28) satisfy all the boundary conditions and all the basic equations except equation (14). It therefore only remains to substitute the known expressions for w' and ϕ into this equation, which gives, after equating to zero the coefficient of exp $(-im\eta)$, the equation

$$\begin{aligned}
&\sum_{t=1}^{\infty} \{(t^2 + m^2)^2 + m^2\bar{q} + k^2t^4/(t^2 + m^2)^2\}A_t \sin t\xi + im\bar{\tau} \sum_{t=1}^{\infty} tA_t \cos t\xi \\
&- Tm^2\{A \cosh m\xi + B \sinh m\xi + \xi(C \cosh m\xi + D \sinh m\xi)\} \\
&- 2Tm\{C \sinh m\xi + D \cosh m\xi\} = 0, \qquad (0 \leqslant \xi \leqslant \pi). \qquad \ldots \quad \ldots \quad (29)
\end{aligned}$$

Equation (29) is now multiplied by $\sin s\xi$ $(s = 1, 2, \ldots)$ and integrated with respect to ξ between 0 and π and it is found that the A_t's satisfy the following infinite and homogeneous system of linear equations,

$$\begin{aligned}
&\{(s^2 + m^2)^2 + m^2\bar{q} + k^2s^4/(s^2 + m^2)^2\} A_s \\
&+ \sum_{t=1}^{\infty} [imb_{st}\bar{\tau} + \{1 + (-)^{s+t}\} k^2a_tc_s] A_t = 0, \qquad (s = 1, 2, \ldots), \qquad \ldots \quad (30)
\end{aligned}$$

where

$$\left.\begin{aligned}
b_{st} &= \begin{cases} 4st/\pi(s^2 - t^2) & \text{if } (s+t) \text{ is an odd integer,} \\ 0 & \text{if } (s+t) \text{ is an even integer,} \end{cases} \\
c_s &= \frac{4ma_s}{(1+\nu)\pi} \cdot \frac{\cosh m\pi - (-)^s}{(3-\nu)\sinh m\pi + (-)^s(1+\nu)m\pi} \cdot
\end{aligned}\right\} \quad \ldots \quad \ldots \quad (31)$$

In general the only solution of these equations is that in which the A_t's are all zero, but this implies that there are no displacements and there is then no question of buckling. A solution for which the A_t's are not all zero is only possible if the infinite determinant whose elements are formed from the coefficients of the A_t's in equation (30) is zero. This is therefore the required criterion for buckling, and the critical stresses are given in terms of the roots of the following infinite determinantal equation,

$$\begin{vmatrix}
z_1, & imb_{12}\bar{\tau}, & 2k^2a_3c_1, & imb_{14}\bar{\tau}, & \ldots \\
imb_{21}\bar{\tau}, & z_2, & imb_{23}\bar{\tau}, & 2k^2a_4c_2, & \ldots \\
2k^2a_1c_3, & imb_{32}\bar{\tau}, & z_3, & imb_{34}\bar{\tau}, & \ldots \\
imb_{41}\bar{\tau}, & 2k^2a_2c_4, & imb_{43}\bar{\tau}, & z_4, & \ldots \\
\ldots & \ldots & \ldots & \ldots & \ldots
\end{vmatrix} = 0, \quad \ldots \quad (32)$$

where

$$z_s = (s^2 + m^2)^2 + m^2\bar{q} + k^2s^4/(s^2 + m^2)^2 + 2k^2a_sc_s. \quad \ldots \quad (33)$$

5.2. *Clamped Edge Conditions.*—The boundary conditions here are

$$u' = v' = w' = \partial w'/\partial\xi = 0, \quad \text{for } \xi = 0, \pi \quad (-\infty < \eta < \infty). \quad \ldots \quad (34)$$

The conditions for the radial displacement are satisfied if

$$\left.\begin{aligned} E &= 0,\\ F &= -\sum_{t=1}^{\infty} tA_t,\\ G &= (1/\pi)\sum_{t=1}^{\infty}\{2 + (-)^t\}tA_t,\\ H &= -(1/\pi^2)\sum_{t=1}^{\infty}\{1 + (-)^t\}t\,A_t. \end{aligned}\right\} \quad \ldots \quad (35)$$

The analysis now is similar to that already given in section 5.1, and it is sufficient to indicate where changes occur in the equations.

Equation (29) becomes

$$\begin{aligned} &\sum_{t=1}^{\infty}\{(t^2 + m^2)^2 + m^2\bar{q} + k^2t^4/(t^2 + m^2)^2\}A_t \sin t\xi + im\bar{\tau}\sum_{t=1}^{\infty} tA_t \cos t\xi\\ &+ m^2(m^2 + \bar{q})(F\xi + G\xi^2 + H\xi^3) - 4m^2(G + 3H\xi) + im\bar{\tau}(F + 2G\xi + 3H\xi^2)\\ &- Tm^2\{A\cosh m\xi + B\sinh m\xi + \xi(C\cosh m\xi + D\sinh m\xi)\}\\ &- 2Tm\{C\sinh m\xi + D\cosh m\xi\} = 0, \quad (0 \leqslant \xi \leqslant \pi), \quad \ldots \quad (36) \end{aligned}$$

and equations (30) are then

$$\begin{aligned} &\{(s^2 + m^2)^2 + m^2\bar{q} + k^2s^4/(s^2 + m^2)^2\}A_s + \sum_{t=1}^{\infty}[m^2(m^2 + \bar{q})\,d_{st}\\ &- 4m^2e_{st} + im(b_{st} + f_{st})\bar{\tau} + \{1 + (-)^{s+t}\}k^2\{c_s(a_t + h_t)\\ &- i_sg_t\}]A_t = 0, \quad (s = 1, 2, \ldots), \quad \ldots \quad (37) \end{aligned}$$

where

$$\left.\begin{aligned} d_{st} &= -(4t/\pi^2s^3)\{2 + (-)^s + (-)^t + 2(-)^{s+t}\},\\ e_{st} &= (2t/\pi^2s)\{2 + (-)^s + (-)^t + 2(-)^{s+t}\},\\ f_{st} &= -(2t/\pi s)\{1 - (-)^{s+t}\} + (12\,t/\pi^3s^3)\{1 - (-)^s\}\{1 + (-)^t\},\\ g_t &= (2\nu t/\pi m^3)\{2 + (-)^t\},\\ h_t &= t/m^2 + 6(2 + \nu)(t/\pi^2m^4)\{1 + (-)^t\},\\ i_s &= 2ms[\{(3 + \nu)s^2 + (1 - \nu)m^2\}\sinh m\pi + (-)^s(1 + \nu)m\pi(s^2 + m^2)]/\\ &\qquad [(1 + \nu)\pi(s^2 + m^2)^2\{(3 - \nu)\sinh m\pi + (-)^s(1 + \nu)m\pi\}]. \end{aligned}\right\} \quad \ldots \quad (38)$$

The infinite determinantal equation corresponding to equation (31) is

$$\begin{vmatrix} N_{11}, & im(b_{12}+f_{12})\bar{\tau}, & N_{13}, & im(b_{14}+f_{14})\bar{\tau}, & \dots \\ im(b_{21}+f_{21})\bar{\tau}, & N_{22}, & im(b_{23}+f_{23})\bar{\tau}, & N_{24}, & \dots \\ N_{31}, & im(b_{32}+f_{32})\bar{\tau}, & N_{33}, & im(b_{34}+f_{34})\bar{\tau}, & \dots \\ im(b_{41}+f_{41})\bar{\tau}, & N_{42}, & im(b_{43}+f_{43})\bar{\tau}, & N_{44}, & \dots \\ \dots & \dots & \dots & \dots & \dots \end{vmatrix} = 0, \qquad (39)$$

where

$$\left.\begin{aligned} N_{st} &= \{(s^2+m^2)^2 + m^2\bar{q} + k^2s^4/(s^2+m^2)^2\}\delta_{st} + m^2(m^2+\bar{q})d_{st} \\ &\quad - 4m^2e_{st} + \{1+(-)^{s+t}\}k^2\{c_s(a_t+h_t) - i_sg_t\}, \\ \delta_{st} &= \begin{cases} 1 \text{ if } s = t, \\ 0 \text{ if } s \neq t. \end{cases} \end{aligned}\right\} \quad \dots \qquad (40)$$

6. *Determination of Critical Shear Stresses.*—Equations (32) and (40) do not yet determine the critical shear stress as they still involve the wavelength as an arbitrary parameter. This must be chosen so that the stress assumes its minimum value, which is then the required critical shear stress. As the order of the determinantal equation is infinite there are an infinite number of critical shear stresses and associated wavelengths, but only the least critical stress is of practical interest.

It is not possible to deal with the infinite determinantal equation as it stands, and attention is perforce confined to a finite determinantal equation derived from a finite number of the A_t's. This means that only the more important of the terms in the expressions for the displacements are considered, and the accuracy of the final results may be estimated from the rate of convergence with increase in the number of terms considered. Approximation to the accurate form of the displacements implies that the panel is subject to additional constraints, and this in turn implies that the critical stress so obtained is in excess of the exact value. The critical stresses obtained from successive order determinantal equations therefore form a monotonic decreasing sequence whose lower bound is the true critical stress. It is found in practice that for the range considered here the convergence is rapid, and it is sufficient at most to consider the fourth-order determinantal equation. This is fortunate, because the computation increases rapidly with the determinant order and is considerable even for the third.

TABLE 1

Variation of $\bar{\tau}$ with $\bar{q}$ and k for Simply Supported Edges

k	n*	$\bar{q} = 0$		$\bar{q} = 10$		$\bar{q} = 25$		$\bar{q} = 40$		$\bar{q} = 50$	
		$\bar{\tau}$	m^2	$\bar{\tau}$	m^2	$\bar{\tau}$	m^2	$\bar{\tau}$	m^2	$\bar{\tau}$	m^2
0	2	11·2	0·58	—	—	—	—	—	—	—	—
	3	10·7	0·64	—	—	—	—	—	—	—	—
	4	—	—	—	—	—	—	—	—	—	—
1	2	12·1	0·75	23·3	0·35	34·2	0·19	42·4	0·13	47·2	0·11
	3	11·5	0·80	19**	0·5**	30·2	0·28	37**	0·2**	41·2	0·17
	4	—	—	—	—	—	—	—	—	—	—
2	2	14·0	1·1	26·6	0·6	39·7	0·35	49·9	0·20	55·6	0·19
	3	12·9	1·1	21	0·7	33·1	0·45	40	0·3	45·3	0·28
	4	—	—	—	—	—	—	—	—	—	—
3	2	16·0	1·4	30·3	0·8	45·6	0·5	57·8	0·35	64·9	0·3
	3	14·6	1·45	23	1·0	36·2	0·65	44	0·5	49·8	0·42
	4	—	—	—	—	—	—	—	—	—	—
4	2	18·2	1·7	33·9	1·1	51·5	0·7	65·8	0·5	74·2	0·45
	3	16·3	1·8	25	1·3	39·4	0·9	48	0·7	54·5	0·57
	4	—	—	—	—	—	—	—	—	—	—
5	2	20·4	2·0	37·8	1·4	57·2	0·9	73·5	0·7	83·1	0·6
	3	17·9	2·1	28	1·5	42·7	1·1	53	0·9	59·1	0·75
	4	17·9	2·1	—	—	41·7	1·2	—	—	56·7	0·85

* n = determinant order.
** The 3rd-order results for $\bar{q} = 10$ and $\bar{q} = 40$ were obtained by interpolation.

TABLE 2

Variation of $\bar{\tau}$ with $\bar{q}$ and k for Clamped Edges

k	n*	$\bar{q} = 0$		$\bar{q} = 10$		$\bar{q} = 25$		$\bar{q} = 40$		$\bar{q} = 50$	
		$\bar{\tau}$	m^2	$\bar{\tau}$	m^2	$\bar{\tau}$	m^2	$\bar{\tau}$	m^2	$\bar{\tau}$	m^2
0	3	17·8	1·5	—	—	—	—	—	—	—	—
	4	—	—	—	—	—	—	—	—	—	—
1	3	18·1	1·6	27**	1·0**	39·9	0·61	48**	0·5**	53·8	0·38
	4	—	—	—	—	—	—	—	—	51·8	0·44
2	3	18·6	1·7	28	1·1	41·4	0·75	50	0·6	56·1	0·47
	4	—	—	—	—	—	—	—	—	—	—
3	3	19·7	1·9	29	1·3	43·5	0·92	53	0·7	59·1	0·59
	4	—	—	—	—	—	—	—	—	—	—
4	3	20·8	2·2	31	1·5	45·9	1·10	56	0·8	62·6	0·70
	4	—	—	—	—	—	—	—	—	—	—
5	3	22·1	2·5	33	1·8	48·2	1·35	59	1·0	66·2	0·90
	4	22·1	2·5	—	—	—	—	—	—	62·0	0·92

* n = determinant order.
** The 3rd-order results for $\bar{q} = 10$ and $\bar{q} = 40$ were obtained by interpolation.

TABLE 3

Variation of $\bar{\lambda}$ with $\bar{q}$ and k ($\bar{\lambda} = 2/m$)

k	Simply Supported Edges					Clamped Edges				
	$\bar{q} = 0$	$\bar{q} = 10$	$\bar{q} = 25$	$\bar{q} = 40$	$\bar{q} = 50$	$\bar{q} = 0$	$\bar{q} = 10$	$\bar{q} = 25$	$\bar{q} = 40$	$\bar{q} = 50$
0	2·500	—	—	—	—	1·672	—	—	—	—
1	2·236	2·86*	3·779	4·48*	4·851	1·581	2·05*	2·561	2·98*	3·247
2	1·907	2·37	2·982	3·54	3·779	1·534	1·91	2·309	2·70	2·915
3	1·661	2·04	2·481	2·83	3·086	1·451	1·76	2·086	2·39	2·604
4	1·491	1·78	2·108	2·43	2·649	1·349	1·62	1·907	2·18	2·389
5	1·380	1·63	1·907	2·14	2·309	1·265	1·49	1·721	1·91	2·107

* The results for $\bar{q} = 10$ and $\bar{q} = 40$ were obtained by interpolation.
Note: These results are obtained from 3rd-order determinants.

TABLE 4

Dimensions of Panels in American Test Specimens

Panel No.	a (in.)	b (in.)	$2h$ (in.)	r (in.)	b/a	$r/2h$	k	$\bar{q}/q$ (in.^{2}/lb)	$\tau/\bar{\tau}$ (lb/in.^{2})	Remarks
1	6	18	0·064	25·6	3	400	7·33	0·388	514	Specimen No. 2 of Ref. 4.
2	6	18	0·064	44·8	3	700	4·20	0·680	514	,, ,, 10 ,, ,,
3	10	30	0·081	65·0	3	800	6·34	1·350	297	Specimen with 10 in. rib pitch of Ref. 3.
4	6	18	0·064	64·0	3	1000	2·94	0·970	514	Specimen No. 18 of Ref. 4.
5	6	18	0·064	76·9	3	1200	2·45	1·167	514	,, ,, 26 ,, ,,
6	12	18	0·064	76·9	1·5	1200	9·77	4·66	128	,, ,, 28 ,, ,,

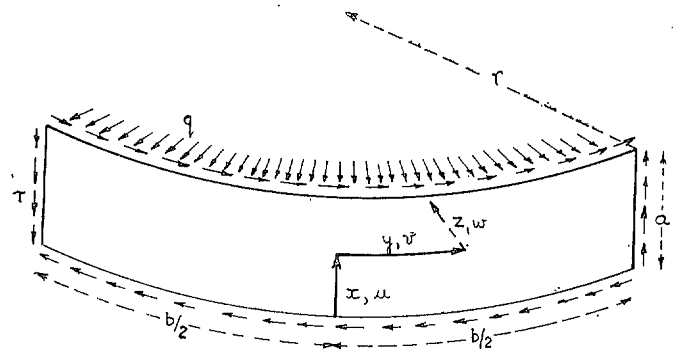

FIG. 1. System of co-ordinate axes and associated displacements.

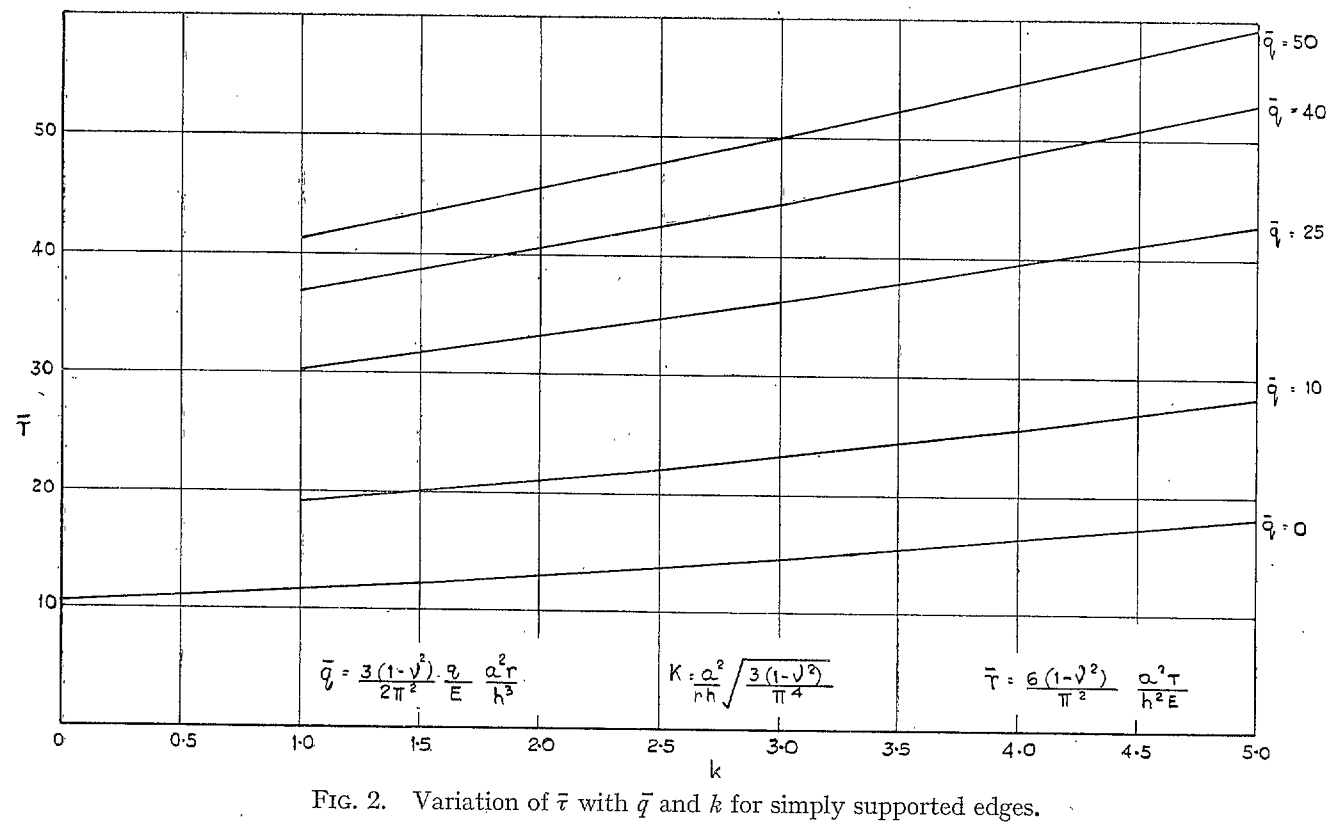

FIG. 2. Variation of $\bar{\tau}$ with $\bar{q}$ and k for simply supported edges.

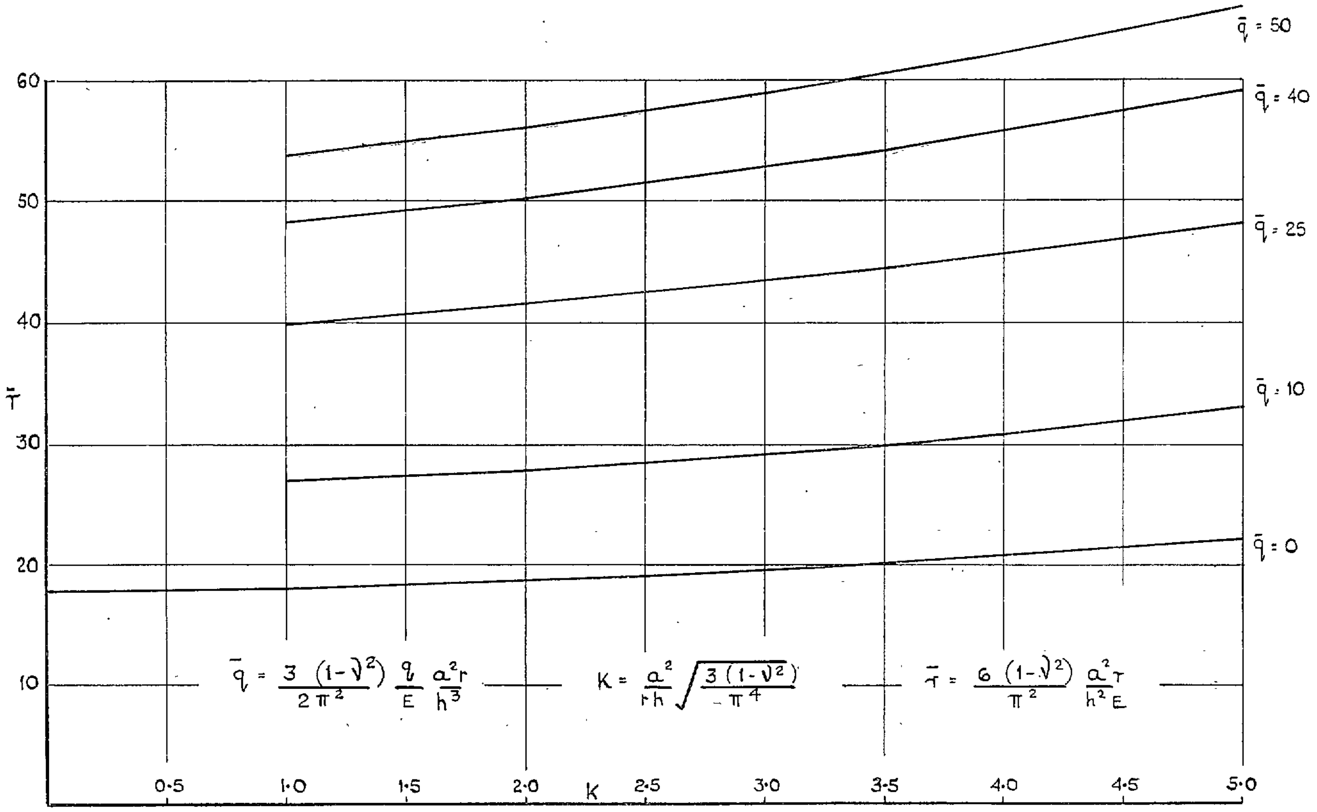

FIG. 3. Variation of $\bar{\tau}$ with $\bar{q}$ and k for clamped edges.

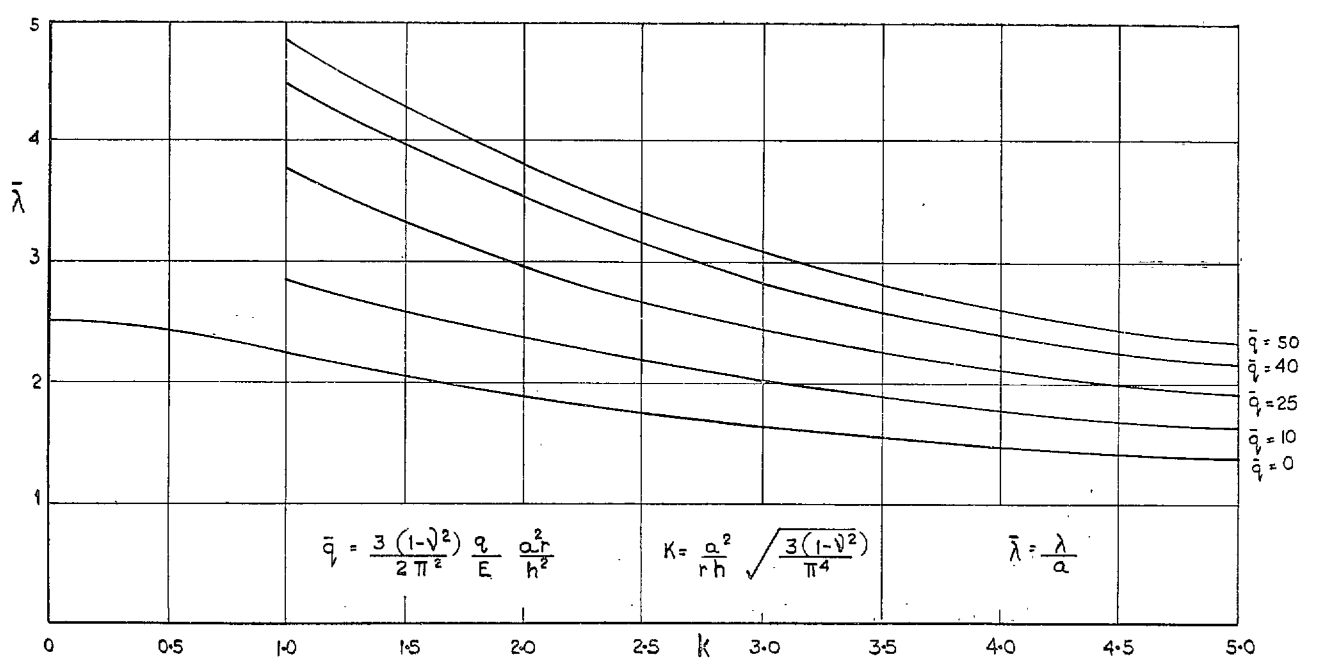

FIG. 4. Variation of $\bar{\lambda}$ with $\bar{q}$ and k for simply supported edges.

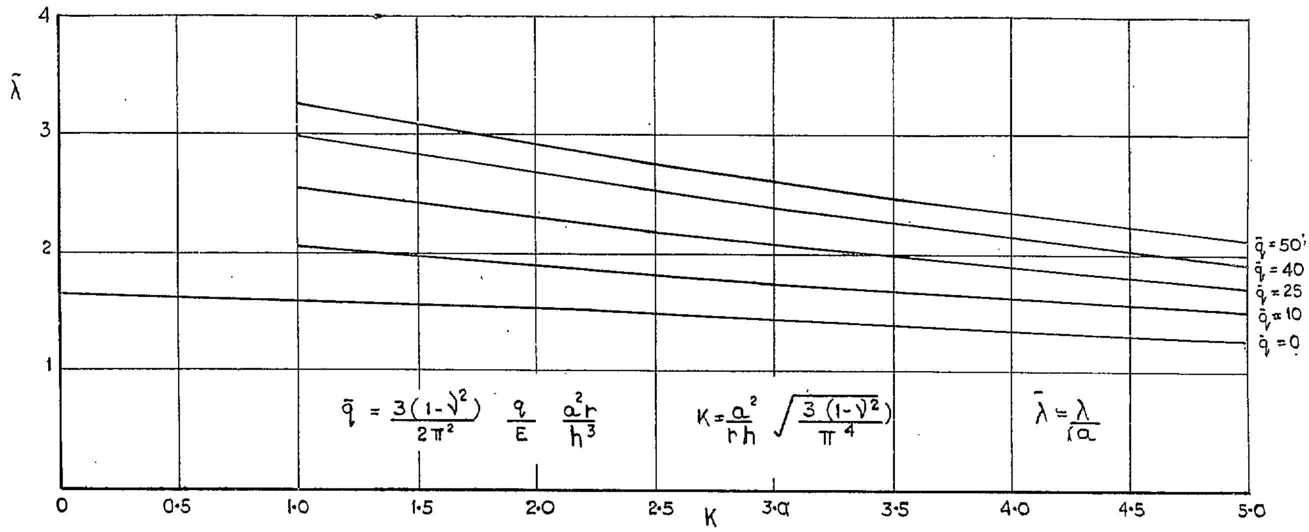

FIG. 5. Variation of $\bar{\lambda}$ with $\bar{q}$ and k for clamped edges.

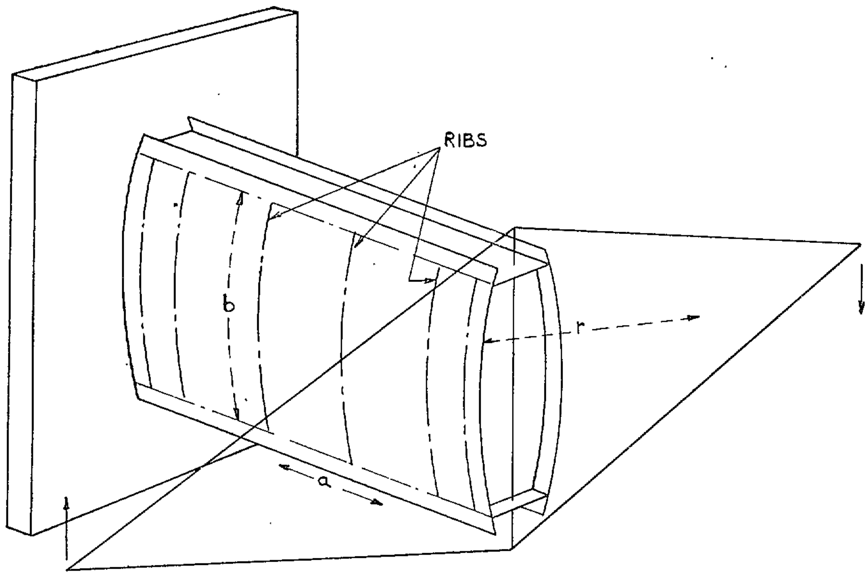

FIG. 6. Diagrammatic representation of American test specimen.

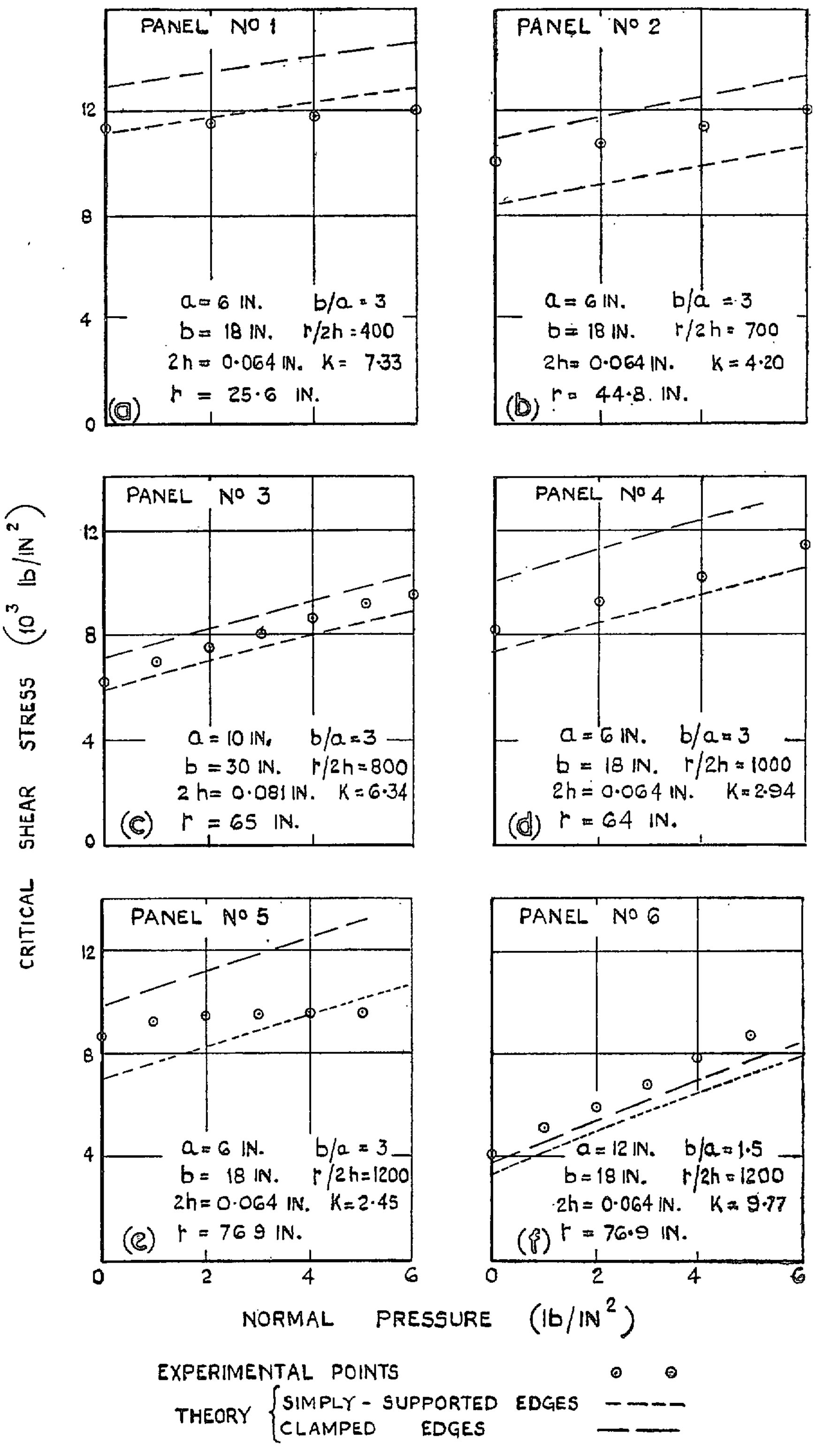

FIG. 7. Comparison between theoretical and American experimental values of critical shear stress.

(22962) Wt. 15-680 K9 10/53 F. M. & S. PRINTED IN GREAT BRITAIN

R. & M. No. 2766
(12,605)
A.R.C. Technical Report

Publications of the Aeronautical Research Council

ANNUAL TECHNICAL REPORTS OF THE AERONAUTICAL RESEARCH COUNCIL (BOUND VOLUMES)

1936 Vol. I. Aerodynamics General, Performance, Airscrews, Flutter and Spinning. 40*s.* (40*s.* 9*d.*)
Vol. II. Stability and Control, Structures, Seaplanes, Engines, etc. 50*s.* (50*s.* 10*d.*)

1937 Vol. I. Aerodynamics General, Performance, Airscrews, Flutter and Spinning. 40*s.* (40*s.* 10*d.*)
Vol. II. Stability and Control, Structures, Seaplanes, Engines, etc. 60*s.* (61*s.*)

1938 Vol. I. Aerodynamics General, Performance, Airscrews. 50*s.* (51*s.*)
Vol. II. Stability and Control, Flutter, Structures, Seaplanes, Wind Tunnels, Materials. 30*s.* (30*s.* 9*d.*)

1939 Vol. I. Aerodynamics General, Performance, Airscrews, Engines. 50*s.* (50*s.* 11*d.*)
Vol. II. Stability and Control, Flutter and Vibration, Instruments, Structures, Seaplanes, etc. 63*s.* (64*s.* 2*d.*)

1940 Aero and Hydrodynamics, Aerofoils, Airscrews, Engines, Flutter, Icing, Stability and Control, Structures, and a miscellaneous section. 50*s.* (51*s.*)

1941 Aero and Hydrodynamics, Aerofoils, Airscrews, Engines, Flutter, Stability and Control, Structures. 63*s.* (64*s.* 2*d.*)

1942 Vol. I. Aero and Hydrodynamics, Aerofoils, Airscrews, Engines. 75*s.* (76*s.* 3*d.*)
Vol. II. Noise, Parachutes, Stability and Control, Structures, Vibration, Wind Tunnels. 47*s.* 6*d.* (48*s.* 5*d.*)

1943 Vol. I. (In the press.)
Vol. II. (In the press.)

ANNUAL REPORTS OF THE AERONAUTICAL RESEARCH COUNCIL—

1933-34	1*s.* 6*d.* (1*s.* 8*d.*)	1937	2*s.* (2*s.* 2*d.*)
1934-35	1*s.* 6*d.* (1*s.* 8*d.*)	1938	1*s.* 6*d.* (1*s.* 8*d.*)
April 1, 1935 to Dec. 31, 1936.	4*s.* (4*s.* 4*d.*)	1939-48	3*s.* (3*s.* 2*d.*)

INDEX TO ALL REPORTS AND MEMORANDA PUBLISHED IN THE ANNUAL TECHNICAL REPORTS AND SEPARATELY—

April, 1950 - - - - - R. & M. No. 2600. 2*s.* 6*d.* (2*s.* 7½*d.*)

AUTHOR INDEX TO ALL REPORTS AND MEMORANDA OF THE AERONAUTICAL RESEARCH COUNCIL—

1909-1949 - - - - - R. & M. No. 2570. 15*s.* (15*s.* 3*d.*)

INDEXES TO THE TECHNICAL REPORTS OF THE AERONAUTICAL RESEARCH COUNCIL—

December 1, 1936—June 30, 1939.	R. & M. No. 1850.	1*s.* 3*d.* (1*s.* 4½*d.*)
July 1, 1939—June 30, 1945.	R. & M. No. 1950.	1*s.* (1*s.* 1½*d.*)
July 1, 1945—June 30, 1946.	R. & M. No. 2050.	1*s.* (1*s.* 1½*d.*)
July 1, 1946—December 31, 1946.	R. & M. No. 2150.	1*s.* 3*d.* (1*s.* 4½*d.*)
January 1, 1947—June 30, 1947.	R. & M. No. 2250.	1*s.* 3*d.* (1*s.* 4½*d.*)
July, 1951. - - - - -	R. & M. No. 2350.	1*s.* 9*d.* (1*s.* 10½*d.*)

Prices in brackets include postage.

Obtainable from

HER MAJESTY'S STATIONERY OFFICE

York House, Kingsway, London, W.C.2; 423 Oxford Street, London, W.1 (Post Orders: P.O. Box 569, London, S.E.1); 13a Castle Street, Edinburgh 2; 39 King Street, Manchester 2; 2 Edmund Street, Birmingham 3; 1 St. Andrew's Crescent, Cardiff; Tower Lane, Bristol 1; 80 Chichester Street, Belfast or through any bookseller.

S.O. Code No. 23-2766